Rewet Temperature Correlations for Liquid-Nitrogen Boiling Pipe Flows across Varying Flow Conditions and Orientations

S. R. Darr[1], J. Dong[1], N. Glikin[1], J.W. Hartwig[2], J. N. Chung[1*]

1. Cryogenics Heat Transfer Laboratory, Department of Mechanical and Aerospace Engineering, University of Florida, Gainesville, FL, 32611-6300, U.S.A.
2. NASA Glenn Research Center, Cleveland, OH, 44135, USA

*Corresponding author. Tel.: 352-392-9607; fax: 352-392-1071

E-mail address: jnchung@ufl.edu (J. N. Chung).

Abstract - In many convective liquid-vapor phase change heat transfer engineering applications, cryogenic fluids are widely used in industrial processes, spacecraft and cryosurgery systems, and so on. For example, cryogens are usually used as liquid fuels such as liquid hydrogen and oxygen in the rocket industry, liquid nitrogen (LN_2) and helium are frequently used to cool superconducting magnetic device for medical applications. In these systems, proper transport, handling, and storage of cryogenic fluids are of extreme importance. Among all the cryogenic transport processes performed in room temperatures, quenching, also termed chilldown, is a unavoidable initial, transient phase-change heat transfer process that brings the system down to the cryogenic condition. The Leidenfrost temperature or rewet temperature that signals the end of film boiling is practically considered the completion point of a quenching process. Therefore, rewet temperature has been considered the most important parameter for the engineering design of cryogenic thermal management systems. As most of the previous correlations for predicting the Leidenfrost temperature and the rewet temperature have been basically developed for water, they are shown to disagree with recent liquid nitrogen pipe chilldown experiments in upward and downward flow directions over a wide range of flow rates, pressures, and degrees of inlet subcooling. In addition to a complete review of the literature, two new correlations are presented in this work, one based on bubble growth and another based on the theoretical maximum limit of superheat. Each correlation performs well over the entire data set.

Keyword: Leidenfrost, rewetting temperature, cryogenics, boiling two-phase flow, line chilldown, quenching, liquid nitrogen.

Nomenclature

$AB\%$	Percent bubble area, m^2
$\Delta AB\%/\Delta t$	Average vapor layer growth rate
c_p	Specific heat, J/kgK
D_b	bubble diameter, m
G	Mass flux, kg/m^2s
g	Gravitational acceleration constant, m/s^2
h	Heat transfer coefficient, W/m^2K

h_{lv}	Latent heat for vaporization, J/kg
k	Thermal conductivity, W/mK
M	Molecular weight, g/mol
N	Atomic number
n	Number of surface cavities
n'	bubble departure frequency, 1/s
P	Fluid pressure, kPa
q''	Heat flux, W/m^2
r	bubble radius, m
Re	Reynolds number
T	Temperature, K
V	Volume, m^3
v	specific volume, m^3/kg
We_D	Weber number, based on inner diameter of tube
x_{eq}	Equilibrium quality

Greek Symbols

α	Thermal diffusivity, m^2/s
β	$1/(k\rho c_p)$, square of the inverse of thermal effusivity
γ	Factor
μ	Dynamic viscosity, Pa·s
ρ	Density, kg/m3
σ	Surface tension, N/m
λ	hydrodynamic wavelength, m
θ	Contact angle
Θ	Nondimensional temperature

Subscripts

agr	average growth rate
ash	available superheat
b	bubble
CHF	Critical heat flux point
cr	at the critical state
f	Property of the liquid
i	interface
l	Liquid state
Leid	Leidenfrost point
min	Minimum heat flux point
ONB	Onset of nucleate boiling
r	reduced by the critical state variable
rsh	required superheat
m	metastable state

sat	liquid saturation state
SS	at steady state chilldown temperature
sub	subcooled
v	vapor state
w	wall surface
wet	rewet point

Abbreviations

AGR	Average Growth Rate
CHF	Critical Heat Flux
GN_2	Gaseous nitrogen
LH_2	Liquid hydrogen
LN_2	Liquid nitrogen
LOCA	Loss of coolant accident
LOX	Liquid oxygen
TC	Thermocouple

1 Introduction

Cryogenic fluids are widely used in many convective liquid-vapor phase-change heat transfer applications. Liquid hydrogen (LH_2) and liquid oxygen (LOX) are commonly used as rocket propellants due to their high specific impulse, whereas liquid nitrogen (LN_2) and liquid helium (LHe) are frequently used to cool superconducting magnetic devices for medical applications and particle accelerators. Of great importance in these systems are the proper transport, handling and storage of cryogenic fluids. When a cryogenic system is first started up by introducing the liquid to the open or closed-loop transfer lines, the pipe walls (~300K) must go through a "chilldown" period to adjust to the liquid cryogenic temperatures (~20K – 80K) prior to reaching a steady operation. Chilldown is the transient process of cooling the ambient system hundreds of degrees to the low temperatures of the cryogen. This is analogous to the quenching of hot surfaces with non-cryogenic liquids, such as water and refrigerants, which occurs in the loss-of-coolant accident (LOCA) scenario in nuclear reactors and in metallurgy heat treatment. The liquid and solid temperatures for these quenching applications are just shifted to higher values than those seen in cryogenic chilldown. However, the same phase-change heat transfer physics is shared by both applications.

The chilldown of a pipe by internal flow of a cryogen is a transient two-phase boiling, conjugate heat transfer problem. The process is characterized by a "curve" that shows the functional relationship between the fluid-solid interface heat flux and the solid surface temperature. Figure 1is a typical curve where the pipe inner surface heat flux, q'', is plotted against the surface degree of superheating, $T_w - T_{sat}$, where T_w is the surface temperature and T_{sat} is the liquid saturation temperature corresponding to the fluid pressure near the surface. In boiling, heat is externally supplied to the heater surface, typically through an electrical resistance heater or through a hotter fluid in a heat exchanger configuration. Thus, heat transfer is controlled independently,

such as the constant wall heat flux condition that results in a steady state process. In this case, boiling is a heat flux (independent variable) controlled process. For the heat flux controlled condition, as the heating rate is progressively increased, the process follows the route of A→B→D, designated here as the “boiling curve”. In order to avoid a severe temperature jump from B→D, boiling applications such as micro-electronics cooling and nuclear power plants usually operate safely below point B in the nucleate boiling regime where the heat transfer coefficients are much higher. The temperature and heat flux at point B are called the dryout temperature and critical heat flux, respectively, to indicate the complete removal of liquid from the heater surface in place of a vapor film. It has also been termed the burnout temperature to imply the catastrophic material failure due to a sudden surface temperature spike that occurs in micro-electronics or nuclear reactor applications when the surface temperature instantly jumps from B→D.

In contrast, during quenching or chilldown, the wall does not have an external source of heat supply. The heat transferring out of the wall can only be supplied internally from the thermal capacity (stored energy) of the solid. This means quenching is a conjugate heat transfer process where the rate of heat transfer is controlled by the surface temperature variation. As a result, the wall surface temperature is the controlling parameter that forces the quenching process to follow the route D→C→B→A. This path is called the “quenching curve”.

If the initial surface temperatures is high enough, film boiling is the first mode of heat transfer encountered in quenching. The heat flux values are very low compared to those in transition and nucleate boiling regimes due to the low thermal conductivity of vapor. Therefore, a majority of the quenching time is spent in the film boiling mode. Once the wall temperature drops below the temperature corresponding to point C in Figure 1, liquid contacts the wall intermittently and sporadically causing an increase in heat transfer. This continues until full liquid contact takes place at the CHF, after which further cooling of the wall takes place by nucleate boiling.

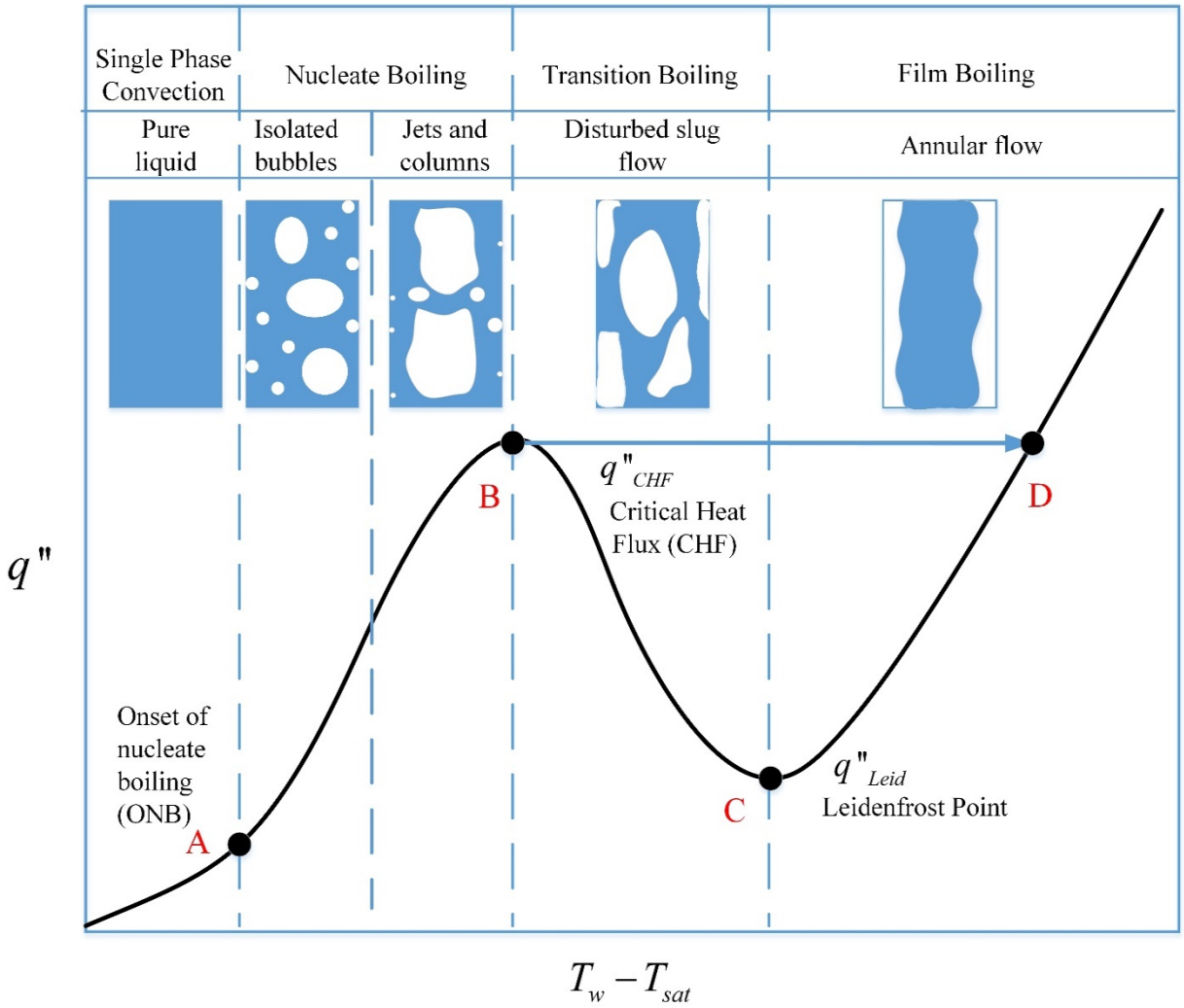

Figure 1. A typical Heat flux vs. wall superheat curve showing both the boiling path (A→B→D) and the quenching path (D→C→B→A).

Historically, many names were used to describe Point C and its temperature at which the boiling mechanism shifts from film boiling to transition boiling. These include the minimum filming boiling temperature, Leidenfrost temperature, rewet temperature, quench temperature, and onset of stable film boiling temperature. The name generally depends upon the method that is used to measure this temperature.

The term “minimum film boiling temperature” is used when it is measured from a pool quenching curve. In this case, a surface at a film boiling temperature is quenched in a pool of liquid until the surface reaches the liquid temperature. The time varying surface temperature curve is used to calculate the heat flux for each temperature measurement with the transient energy equation. The heat flux at the end of film boiling and the beginning of transition boiling (point C in Figure 1) is a local minimum in the quenching curve. Therefore, the temperature corresponding to this heat flux is the minimum film boiling temperature.

In the technique of measuring droplet vaporization times, this temperature is called the Leidenfrost temperature. This method consists of placing liquid droplets on a heated surface and measuring the time it takes to completely vaporize the droplet. The heated surface is held at a

constant temperature and the presence of the droplet only slightly alters the surface temperature in the close proximity of the droplet. This test is repeated for several surface temperatures spanning the quenching curve. The surface temperature that causes the longest droplet evaporation time is designated as the Leidenfrost temperature. The actual Leidenfrost temperature is lower than the surface temperature setting, since the location of the surface in contact with the droplet is temporarily cooled below the temperature of the majority of the surface. This is usually accounted for by applying an adjustment to the measured value [1].

In the cases of cryogenic pipe chilldown and reflooding of a nuclear reactor, the temperature is typically called the rewet or quench temperature. This is similar to the first method in that a time-variant wall temperature curve is used to calculate a q'' vs $T_w - T_{sat}$ curve. For low flow rates, if the test is held at a fairly constant flow rate, the rewet temperature will occur at the minimum heat flux during film boiling. However, for high enough flow rates it has been shown that the heat flux can actually begin to increase during film boiling as the temperature approaches the rewet temperature, as shown in Figure 2. This has been attributed to an enhancement in film boiling heat transfer caused by the presence of a large liquid core flowing through the center of the tube that thins the vapor layer. As the wall temperature is decreased the liquid core becomes larger, thinning the vapor layer to ever smaller values. Waves in the liquid-vapor interface are able to bring liquid in very close proximity to the surface, greatly increasing the heat transfer [2]. Another conceivable mechanism for enhanced film boiling at high flow rates is that the highly turbulent two-phase mixture introduces liquid droplets into close contact with the wall This occurrence has been designated as “precursory cooling” in studies on LOCA [1]. For this reason, the minimum heat flux cannot necessarily be designated as the temperature dividing the film and transition boiling regimes for pipe quenching scenarios. For most liquids and flow conditions, there still exists a noticeable jump in heat flux that makes the division between the film and transition boiling regimes apparent, which is designated as the rewet temperature. The temperature at this point can be identified by either inspecting the T_w vs. t curve or q''_w vs. t curve looking for a sharp change in slope. This is shown for a low and high mass flux LN_2 pipe chilldown test in Figure 2.

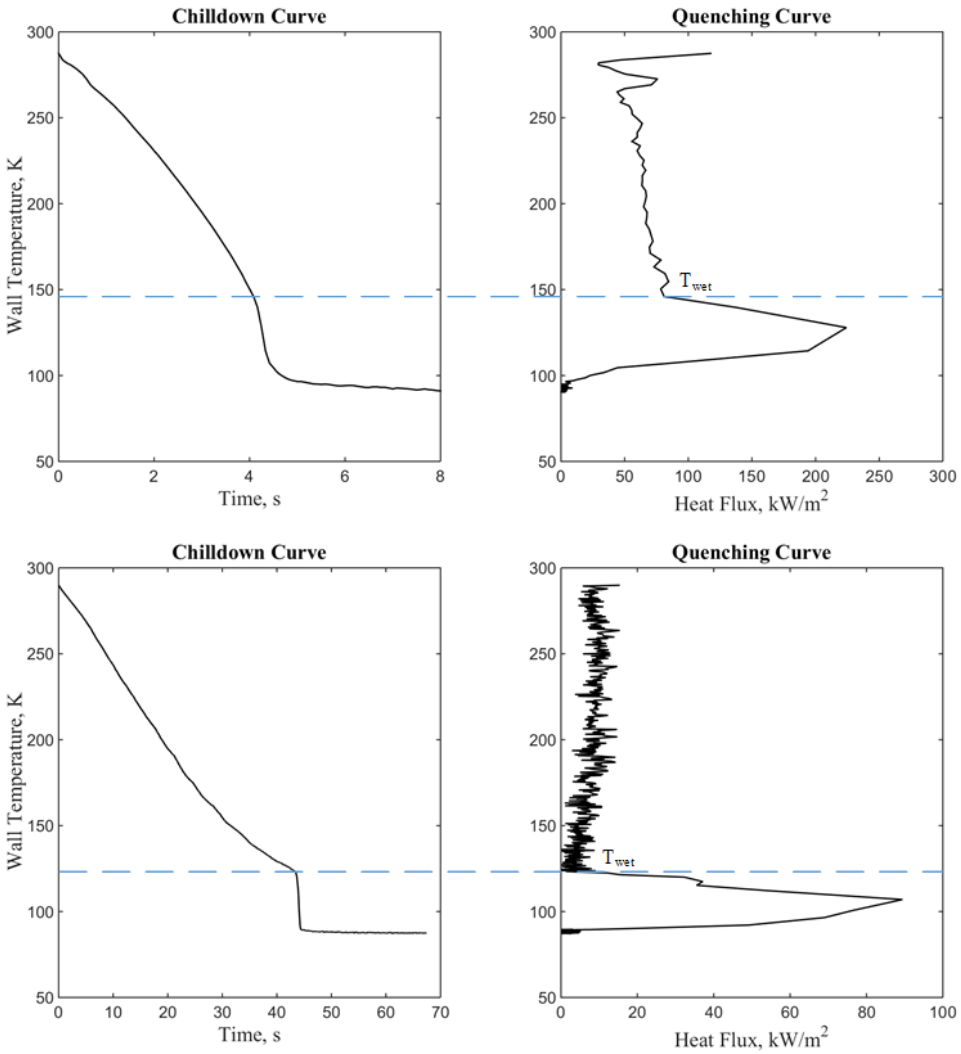

Figure 2 Typical chilldown and quenching curves, top : high flow rate and bottom : low flow rate. The blue dotted lines show the division between the film and transition boiling regimes.

It is not necessarily the case that all methods will produce the same measurement for the temperature that divides the film and transition boiling regimes. It is expected that the minimum film boiling temperature will correspond to the actual Leidenfrost temperature for saturated conditions, but it has been shown that there is a difference if the liquid is subcooled. Whereas subcooling causes an increase in the rewet temperature for pool quenching [3], subcooling has little effect on the Leidenfrost temperature of evaporating droplets [4]. Also, the influence of bulk flow across the surface that is present in reflooding or chilldown will cause the rewet temperature to be higher than what is measured with the Leidenfrost technique.

The goal of this paper is to provide a new correlation for the rewet temperature, T_{wet} developed based on recent pipe chilldown experiments with LN_2 [5, 6]. Previous theories and correlations for the minimum film boiling temperature, the Leidenfrost temperature, and the rewet temperature are studied and compared to the data in order to determine an appropriate form for the new correlation.

2 Previous modeling efforts

Existing models for T_{wet} can, for the most part, be divided into three main groups that were developed from different theories. These include models based on hydrodynamic theory, maximum limit of superheat, and heterogeneous bubble nucleation and growth.

2.1 Hydrodynamic models

Berenson [7] presented a model to predict the minimum film boiling temperature for boiling on top of a flat, horizontal surface. It was noticed from film boiling experiments with n-pentane and carbon tetrachloride that the bubbles would grow from the vapor film, detach and rise away from the film. This process of bubble growth would repeat itself in regular intervals. The bubbles that grew over the surface formed a square lattice. Therefore the analysis started from an idealized situation of a hemispherical bubble growing out of a flat, thin vapor layer. The minimum film boiling temperature was found by:

$$\Delta T_{min} = T_{min} - T_{sat} = \frac{q''_{\min}}{h_{min}} \tag{1}$$

The expressions for $q''_{\min}$ and h_{min} were derived separately but with similar assumptions. The derivation of $q''_{\min}$ was first given by Zuber [8] and goes as follows. It was postulated that $q''_{\min}$ was the heat flux that produced the minimum rate of vapor removal from the vapor film that could keep up with the bubble departure rate. Below this heat flux, the amount of vapor leaving the film by bubble departure would exceed what been vaporized at the liquid/vapor interface. This would allow the liquid to wet the surface. This led to the equation:

$$q''_{\min} = \frac{\pi}{6}\rho_v D_b^3 h_{lv} n' \tag{2}$$

The bubble diameter, D_b, was found visually from experiments with n-pentane and carbon tetrachloride. The bubble departure frequency per unit area, n', was found by considering hydrodynamic theory. When a liquid resides on top of a vapor, any disturbance in the interface grows in time. From perturbation analysis derived earlier from Taylor [9] and the general solution to the irrotational flow kinematic equation, expressions were derived for the growth rate of the interface as a function of the surface tension, the liquid and vapor densities, acceleration due to gravity, and the wavelength of the disturbance. It was argued that the disturbance wavelength that maximized the bubble growth rate would be the dominant, visible wavelength in film boiling. It was also assumed that the velocity of the vapor and the vapor film thickness are negligibly small at the minimum heat flux, which simplified the equation for the interface growth rate. The disturbance wavelength corresponding to the maximum growth rate of the interface was found to be:

$$\lambda = 2\pi\sqrt{\frac{3\sigma}{g(\rho_v - \rho_l)}} \tag{3}$$

This being the dominant wavelength, it followed that 4 bubbles would depart from a square area of λ^2 for the time period for a single bubble to grow and depart. It was assumed that this period was equal to four times the time it would take for the interface disturbance to grow to a height equal to D_b. This gave an expression for n' that could be plugged into Eq. (2). Based on the above discussion, Zuber [8] gave the following equation for $q''_{\min}$,

$$q''_{min} = 0.35\rho_v h_{lv}\left(\frac{g(\rho_v-\rho_l)}{(\rho_v+\rho_l)}\right)^{1/2}\left(\frac{\sigma}{g(\rho_v+\rho_l)}\right)^{1/4} \quad (4)$$

The constant, 0.35, related to the initial height of the interfacial disturbance, was corrected by Berenson [10] by fitting to data so that Eq. (4) became:

$$q''_{min} = 0.09\rho_v h_{lv}\left(\frac{g(\rho_v-\rho_l)}{(\rho_v+\rho_l)}\right)^{1/2}\left(\frac{\sigma}{g(\rho_v+\rho_l)}\right)^{1/4} \quad (4)$$

The expression for h_{min} was derived by Berenson [7] who incorporated the Taylor hydrodynamic wave instability theory into the film boiling model for a horizontal tube developed by Bromley [11] and the pool film boiling heat transfer coefficient is given below:

$$h_{\min} = 0.425\left[\frac{k_v^3 h_{lv}\rho_v g(\rho_v-\rho_l)}{\mu_v\Delta T_{\min}\sqrt{\frac{\sigma}{g(\rho_v+\rho_l)}}}\right]^{1/4} \quad (5)$$

Combining Eqs. (1), (4), and (5), the expression for the minimum film boiling temperature based on the Berenson model (Eq. 4) was found to be:

$$T_{wet,Ber} = 0.127\frac{\rho_v h_{lv}}{k_v}\left[\frac{g(\rho_l-\rho_v)}{\rho_l+\rho_v}\right]^{2/3}\left[\frac{\sigma}{g(\rho_l-\rho_v)}\right]^{1/2}\left[\frac{\mu_v}{g(\rho_l-\rho_v)}\right]^{1/3} \quad (6)$$

This model performed well for the n-pentane and carbon tetrachloride pool quenching data. However it was later found that this model performed poorly for Leidenfrost data with many fluids including cryogens [12, 4].

Henry [13] developed a correlation using Berenson's model and including terms for a transient wetting effect and a microlayer evaporation effect. It was suggested by evidence from previous experiments that during horizontal film boiling the liquid momentarily contacts the wall by snapping back towards the wall after a bubble departs. After the liquid contacts the wall, the wall temperature is lowered to the interface temperature. The superheat of the wall immediately boils off a small microlayer of liquid while the wall temperature continues to drop. Generated vapor then pushes the rest of the liquid away from the wall. The effect of this behavior is that the wall temperature near the minimum film boiling temperature is transient instead of isothermal. If the temperature drops below that predicted by Eq. (6), the liquid is able to fully wet the surface to begin transition boiling. Considering the liquid and wall as infinite slabs in contact, the interface temperature is different from the wall temperature before contact. Two dimensionless parameters were introduced for the transient wetting and the microlayer evaporation effects. The correlation, which was fitted to pool quenching data both at saturated and subcooled conditions from several solid materials and several fluids including water, n-pentane, ethanol, sodium, potassium, and Freon-11, was:

$$T_{wet} = T_{wet,Ber} + 0.42\left[\sqrt{\frac{\beta_w}{\beta_l}}h_{lv}/\left[c_{p,w}\left(T_{wet,Ber}-T_{sat}\right)\right]\right]^6\left(T_{wet,Ber}-T_{sat}\right) \quad (7)$$

where $T_{wet,Ber}$ is the rewet temperature calculated from the Berenson model (Eq. 6). The first parameter on the right hand side of Eq. (7), $\beta = 1/(k\rho c)$, is thermal liqu. This ratio of thermal effusivities of the liquid and wall was previously noticed as an influential parameter on the minimum film boiling temperature by Kalinin [2] and Baumeister and Simon [4]. If the ratio is very large, which is very possible for low-conductivity solids such as glass and high conductivity liquids like liquid metals, there will be a significant difference between Eq. (7) and Eq. (6). $T_{wet,Ber}$ is calculated from Eq. (6). Additionally, if the heat of vaporization of a liquid is large compared to the sensible heat change of the wall material from the liquid saturation temperature to the wall temperature, it will result in a significant difference in $T_{wet,Ber}$ and T_{wet}. Even though the correlation did fairly well for many liquid-solid combinations at both saturated and subcooled temperatures, it was noted that Berenson's model probably does not apply to cryogenic liquids since the homogeneous nucleation temperature for cryogens is actually lower than the prediction from Eq. (6)., which is not the case for water, liquid metals, and refrigerants.

Iloeje et al. [14] presented a minimum film boiling temperature correlation for pipe flow quenching, which applied terms to Berenson's equation for mass flux and equilibrium quality:

$$\Delta T_{min} = 0.29\left(T_{\min,Ber} - T_{sat}\right)\left(1 - 0.295 x_{eq}^{2.45}\right)\left(1 - 0.279 G^{0.49}\right) \tag{8}$$

where G is mass flux with units of kg/m^{2}s and x_{eq} is equilibrium quality. Data used to fit the correlation was obtained with water at high pressure and high mass fluxes through a short, 1.25 cm diameter Inconel tube. Berenson's equation was chosen from the argument that the minimum film boiling temperature of the water data was higher than that predicted by the maximum limit of superheat, and in some instances even higher than the critical temperature. Higher mass fluxes resulted in larger values for the minimum film boiling temperature. This was attributed to higher amounts of mixing of the flow, which reduced the average vapor temperature, and higher momentum of liquid droplets that would approach the wall to wet it prematurely. Higher equilibrium qualities were shown to reduce the minimum film boiling temperature, due to there being less liquid droplets carrying momentum to the walls and higher average vapor temperatures. The quality was able to be controlled in this experiment with a preheating section, which is not common in quenching applications such as cryogenic chilldown. For chilldown, the equilibrium quality naturally evolves from the conjugate heat transfer between the pipe and the fluid, which depends on the mass flux, the fluid properties, the tube length and diameter, and the temperatures of the liquid, vapor, and wall. Therefore it is likely that a minimum film boiling temperature for cryogenic chilldown does not need a quality term, since any effect of quality can be accounted for by the other independent variables.

2.2 Maximum limit of superheat models

Spiegler et al. [15] proposed that the surface temperature at the onset of stable film boiling could be estimated as the maximum possible superheat that a liquid could be maintained in a metastable state, which was earlier derived by Temperley [16]. In Temperley's paper, the main focus is the tensile strength of the liquid. However, from this paper came the first analysis of the end of a metastable liquid state due to depressurization. For a liquid described by the Van Der Waals equation of state, normalized by the critical state:

$$P_r = \frac{8T_r}{3V_r - 1} - \frac{3}{V_r^2} \tag{9}$$

This equation of state predicts a discontinuous change of state if there is any region for which $\left(\partial P/\partial V\right)_T$ is positive. This implies that when $\left(\partial P/\partial V\right)_T$ is set to zero, the expression that follows describes a fluid at the limit of metastable state:

$$\frac{24T_{r,m}}{\left(3V_{r,m}-1\right)^2}=\frac{6}{V_{r,m}{}^3} \tag{10}$$

Plugging Eq. (10) into (9):

$$P_{r,m}=\left[3-\frac{2}{V_{r,m}}\right]\frac{1}{V_{r,m}^2} \tag{11}$$

Eqs. (10) and (11) determine the conditions at the limit of metastable state. Temperley [16] set $P_{r,m}$ to zero, giving the result of:

$$T_{r,m}=27/32 \tag{12}$$

The physical meaning of this temperature is that for a liquid suddenly brought to a pressure of zero, the liquid should be at a temperature below $T_m = (27/32)T_c$ in order to keep it from instantly vaporizing. Temperley found that Eq. (12) compared well with superheated data at atmospheric pressure. Spiegler et al. [17] first used Eq. (12) to predict the foam limit in a study on bubble chambers. It was shown that instead of using $P_{r,m} = 0$, the pressure can be set to the operating pressure of the bubble chamber to get marginally better agreement with data. This had the effect of increasing $T_{r,m}$ a few percent above the constant of 27/32 predicted by Eq. (12). The model agreed well with bubble chamber data from many fluids including hydrogen. Spiegler [15] then applied the same equation to predict the surface temperature at the onset of stable film boiling, arguing that for pressures much less than the critical pressure the assumption of $P_{r,m} = 0$ should be a good approximation. The model compared well with pool quenching and Leidenfrost droplet data with many fluids including LN_2.

Lienhard and Schrock [18] tried a similar method as Spiegler [17] but looked at the effect of raising the liquid temperature at constant pressure instead of decompressing the liquid at constant temperature. At the beginning, the liquid is in stable equilibrium at a reduced temperature and pressure of $T_{r,sat}$ and $P_{r,sat}$. The liquid is then heated to a max temperature without boiling, and pressure is kept constant. $T_{r,m}$ is the reduced temperature at which $\left(\partial P_r/\partial V_r\right)_T = 0$ for this pressure. Along with this theory, an equation relating $P_{r,sat}$ to $T_{r,sat}$ was derived with some assumptions and the van der Waals equation of state. This model was later compared to boiling data on rapidly heated wires, where the boiling curve path A→B→D was taken, with multiple fluids over a wide range of temperatures and pressures [19]. Because the forward boiling method was used, the measured temperature at the onset of film boiling was likely the dryout temperature. The model overpredicted the value of $\Delta T_{r,m} = T_{r,m} - T_{r,sat}$ measured from the data for a given $P_{r,sat}$. It was found that when plotting the data of $\Delta T_{r,m}$ versus $T_{r,sat}$, a simple correlation could be fit to the data with fine accuracy:

$$\Delta T_{r,m}=0.905-T_{r,s}+0.095T_{r,s}^8 \tag{13}$$

In an attempt to correlate the minimum film boiling heat flux and temperature data for vertical flow of LN_2 through a pipe, Simon and Simoneau [20] suggested the constant in Eq. (12) should be modified to a value between 0.872 and 0.916. However, this data was obtained in an electrically-heated tube and was carried out in such a way that the boiling path (D→B→A) was followed rather than the quenching path (D→C→B→A). Therefore this correlation is not

necessarily a reliable prediction of the true minimum film boiling temperature for cryogenic chilldown.

Baumeister and Simon [4] presented a modified version of Eq. (12) to predict the Leidenfrost temperature that accounted for two separate effects. The first effect pertains to the small decrease in the local surface temperature near a droplet during a Leidenfrost experiment. When such an experiment is carried out, the temperature of the heating plate is set to a certain constant value. The droplet is then placed on the plate and boiled off, and there is a small dip in temperature in the vicinity of the droplet below the set temperature of the plate. It is noted that this transient temperature is normally not recorded by the experimenter. Most likely the temperature of the plate is measured far from the droplet location where no temperature drop is measurable. This means that the method of normally measuring the Leidenfrost temperature is not accurate and it gives a higher value than the actual Leidenfrost temperature. Instead of a correlation with β, as in Eq. (7) from Henry [13], the drop in temperature at the surface is accounted for by solving the transient conduction equation for two infinite slabs. An assumption is that the droplet can be modeled as an infinite slab and that it is in contact with the solid surface. This simplifies the conduction equation to one dimension, and it is noted that this assumption causes the temperature drop to be overestimated since radial conduction through the solid plate away from the droplet will reduce this temperature drop. The solution for the nondimensional temperature reduction is:

$$\Theta = \frac{T_w - T_l}{T_{w,0} - T_l} = \exp\left(\frac{h^2 t}{k_w \rho_w c_w}\right) \operatorname{erfc}\left(\sqrt{\frac{h^2 t}{k_w \rho_w c_w}}\right) \tag{14}$$

Where $T_{w,0}$ is the initial solid temperature. For relatively large values of the group $\beta_w = 1/(k_w \rho_w c_w)$, such as for aluminum and copper, Θ is close to 1. For smaller values of β, as is the case for stainless steel and even more so for glass, Θ can become significantly less than 1. A value of 3.06×10^6 (in SI units) was assumed for h^2t, using a heat transfer coefficient typically measured at the departure of nucleate boiling and droplet evaporation times which were measured around 0.01s.

The second effect that was included was that of the combined solid and liquid surface energies. Cryogenic Leidenfrost data agreed well with Eq. (12) and it was claimed that this was due to the very low surface tension of cryogens. For other fluids like water and liquid metals, the Leidenfrost temperature was overestimated by Eq. (12). To account for this, the data was correlated with the ratio of the surface energy of the solid, which was estimated as ρ_w/A_w, to the surface energy of the liquid, i.e. the surface tension.

Combining the two effects, the proposed correlation for the Leidenfrost temperature was, with the denominator in SI units:

$$T_{Leid} = \frac{0.844 T_{cr}\left(1 - \exp\left\{-0.52\left[10^4 \left(\rho_w / N_w\right)^{4/3} / \sigma\right]^{1/3}\right\}\right) - T_{sat}}{\exp\left[3.06\times10^6 \beta_w\right] \operatorname{erfc}\left[1751.5 \beta_w^{1/2}\right]} + T_{sat} \tag{15}$$

It should be noted that this correlation is for the *measured* Leidenfrost temperature, which, as discussed earlier, is slightly higher than the actual Leidenfrost temperature. If the actual Leidenfrost temperature was measured in an experiment or if the slab was at isothermal conditions in the vicinity of the droplet then Eq. (15) can be simplified to:

$$T_{Leid} = 0.844 T_{cr}\left(1 - \exp\left\{-0.52\left[10^4 \left(\rho_w / N_w\right)^{4/3} / \sigma\right]^{1/3}\right\}\right) \tag{16}$$

Bernardin and Mudawar [21] noted that the main issue with this model is probably that it was not explicitly clarified how the average heat transfer coefficient in Eq. (14) was determined.

In an attempt to provide a useful correlation to implement in a pipe flow quenching numerical simulation, De Salve and Panella [22] modified the correlation by Baumeister and Simon [4] to include a mass flux term in the same way that Iloeje et al. [14] modified the correlation by Berenson [7]:

$$T_{Leid} = \frac{0.29\left(0.844T_{cr} - T_{sat}\right)}{\exp\left[3.06\times10^{6}\beta_{w}\right]\operatorname{erfc}\left[1751.5\beta_{w}^{1/2}\right]}\left(1+0.279G^{0.49}\right)+T_{sat} \tag{17}$$

Additionally, the constant 0.29 is adopted from Eq. (8) and the effect of the liquid and solid surface energies was removed from the equation. The data was found to agree with water quenching data.

2.3 Heterogeneous nucleation and bubble growth model

Yao and Henry [23] suggested that the hydrodynamic instability is one of the sufficient mechanisms to initiate the onset of the Leidenfrost point, but it is not the only necessary condition. They proposed that another sufficient condition is the homogeneous nucleation of the superheated liquid that is brought to the proximity of the hot wall by the two-phase flow actions. Between hydrodynamic instability and homogeneous nucleation, the one that requires smaller wall temperature to establish the wall rewetting would prevail. Cryogenic liquids generally demand lower levels of superheat to initiate homogeneous nucleation when compared to hydrodynamic instability. As a result, homogeneous nucleation may be the more likely mechanism responsible for the rewetting to take place.

Bernardin and Mudawar [24] developed a model of the Leidenfrost temperature where the controlling mechanism is the nucleation and growth of bubbles from the cavities of the solid surface, also known as heterogeneous boiling. This is in contrast to the maximum limit of superheat which represents boiling in a pool of liquid, termed homogeneous boiling. In its essence, the model from Bernardin and Mudawar [24] describes a situation starting in nucleate boiling in which the bubble generation becomes so fast that a continuous vapor film forms and covers the surface in a short time. This model can be broken into three parts. First, a model was given for the thermally controlled nucleate boiling process. The required superheat in the liquid to initiate bubble growth was found assuming that the cavities in the solid surface are conical and that the bubbles grow as hemispheres from the surface, and then integrating the Clausius-Clapeyron relation along the saturation line to obtain the required superheat for a given bubble radius r:

$$T_{rsh} = \exp\left(\frac{2\sigma v_{lv}}{rh_{lv}}\right)T_{sat} \tag{18}$$

The physical meaning of this model is that once a bubble is formed in a surface cavity, the temperature at the top of a bubble hemisphere should be as high as or higher than T_{rsh} for the bubble to continue to grow and not collapse. Next, the thermal boundary layer in the liquid next to the heated solid was solved assuming the liquid and solid were infinite slabs brought into contact instantaneously, the same assumption used by Baumeister and Simon [4]. From this assumption, the transient one-dimensional conduction equation could be used, resulting in the solution for the available superheat at a distance y normal from the surface and time t from the start of the liquid-solid contact:

$$T_{ash} = T_i + (T_l - T_i)\, erf\left(\frac{y}{2\sqrt{\alpha_l t}}\right) \tag{19}$$

Where T_i is the interface temperature, equal to:

$$T_i = \frac{\beta_w^{1/2} T_w + \beta_l^{1/2} T_l}{\beta_w^{1/2} + \beta_l^{1/2}} \tag{20}$$

In order for a bubble generated at a cavity to grow, the available superheat, T_{ash}, at the bubble edge (y = r) must be greater than or equal to the required superheat, T_{rsh}. To set this requirement, Eq. (18) and Eq. (19) are set equal (and y is set equal to r) so that:

$$T_i + (T_l - T_i)\, erf\left(\frac{r}{2\sqrt{\alpha_l t}}\right) = \exp\left(\frac{2\sigma v_{lv}}{r h_{lv}}\right) T_{sat} \tag{21}$$

Solving for r in Eq. (21) produces two roots which represent a minimum and maximum bubble radii (rmin, rmax) that can be supported by the thermal boundary layer, r_{min} and r_{max}.

The second part of the model was characterizing the cavity size distribution of the heated surface. Scanning electron microscopy of aluminum, nickel, and silver showed that the number of cavities per square unit area for any cavity size could be described by the empirical equation:

$$dn = a_1 \exp(-a_2 r)\, dt \tag{22}$$

Coefficients a_1 and a_2 were dependent on the material. Integrating Eq. (22) from r_{min} to r_{max} found from Eq. (21), the cumulative number of activated cavities per unit area at a given time are:

$$nc = \psi \frac{a_1}{a_2}\left\{\exp\left[-a_2 r_{\min}(t)\right] - \exp\left[-a_2 r_{\max}(t)\right]\right\} \tag{23}$$

The coefficient ψ is a number less than one to take into account the fact that not all cavities in the radius range are activated due to several identified cancellation effects. For example, some cavities are steeper than the advancing contact angle causing vapor to become trapped inside.

The last part of the model involved determining what limiting condition would produce a full coverage of the surface with a vapor blanket. It was noted that the initial stage of bubble growth, known as inertia-controlled bubble growth, is orders of magnitude faster than that the latter stage which is controlled by the thermal boundary layer. Using this argument, it was assumed that all bubbles with an initial radius less than r_{max} instantly grew to the value of r_{max}, after which growth only occurred by the growth of the thermal boundary layer. With this assumption, a simple formula to calculate the percent area of bubble coverage could be formed:

$$AB\%(t) = nc_a(t)\, \pi r_{\max}^2(t) = \psi \frac{a_1}{a_2}\left\{\exp\left[-a_2 r_{\min}(t)\right] - \exp\left[-a_2 r_{\max}(t)\right]\right\} \pi r_{\max}^2(t) \tag{24}$$

The fraction ψ was found empirically to be 0.05 by comparing the model percent vapor layer growth to one droplet boiling data point with water on aluminum in the nucleate boiling regime. The vapor area coverage percentage measured visually was well predicted by the model with ψ = 0.05. It was assumed that this value could be used for all conditions that were tested.

Eq. (24) predicts that, eventually, for any wall superheat the percent area coverage will reach 100 percent. This, however, is known to not be true because bubbles release from the surface. It was determined that the Leidenfrost temperature, taken as the interface temperature from Eq. (20), had to be evaluated from the average growth of AB% over time. It was found that the predicted Leidenfrost temperature agreed with water data on aluminum best for an average growth rate of $\Delta AB\%/\Delta t = 0.05$. Using this value for $\Delta AB\%/\Delta t$, the model was able to predict the Leidenfrost

temperature within a few degrees for water on all three surfaces and FC-72 on aluminum. For acetone on aluminum the predicted Leidenfrost temperature was 42K lower than the measured value.

2.4 Other models and correlations

Segev and Bankoff [25] suggested a model according to the minimum film boiling mechanism that is based on the adsorption characteristics of the system. They proposed that the wetting process is characterized by a precursor, non-evaporating film. They further claimed that as the surface temperature increases the film thickness decreases, with a sharp decrease at a temperature threshold determined by the heat of adsorption. The minimum film boiling temperature is assumed to be the temperature at which only one monolayer exists. They reported that predicted values were in fair agreement with experimental results for different systems.

Carbajo [1] presented an empirical rewet temperature correlation for pipe flow quenching that applied several factors corresponding to different influences, including transient contact between the liquid and solid, surface roughness, mass flux, and liquid subcooling. The equation took the form:

$$\Delta T_{\min} = \Delta T_{\min,iso}\left(1+\frac{\beta_l}{\beta_s}\gamma\right)\left(1+0.1G^{0.4}\right)+a\Delta T_{sub} \tag{25}$$

The surface condition factor γ accounts for effects of surface roughness, surface oxidation, and contact angle. An expression for coefficient *a* was fit to the data:

$$a = \frac{4180}{c_{p,l}}\frac{h_{lv}}{h_l}\left\{\beta\frac{h_{lv}}{c_{p,w}}\Delta T_{\min,iso}\right\}^{0.1} \tag{26}$$

$\Delta T_{min,iso}$ is the minimum film boiling temperature difference for an isothermal surface without transient contact. Data with several fluids and high thermal capacity surfaces were used to fit an empirical relationship for $\Delta T_{min,iso}$. This equation, however, was found to severely overpredict $\Delta T_{min,iso}$ for cryogenic liquids and therefore was considered unsuitable for the interest of the current work. However, the factors included in Eq. (25) help to identify the expected effects of the many influential parameters for pipe flow quenching.

3 Comparison to Experiment Results

ΔT_{wet}, which is the same as ΔT_{min} and defined as $T_{wet} - T_{sat}$, was found to depend primarily on mass flux, as shown in Figure 3 which is taken from authors' own data for LN_2 chilldown experiment [5, 6]. The circles are for upward flows and the triangles are for downward flows. The scatter in this plot showed no noticeable correlation with pressure or inlet subcooling for a given mass flux. At the lowest mass flux values tested, ΔT_{wet} was measured from 30 to 43K. At the highest mass flux values ΔT_{wet} was measured between 45 and 50K. At low to moderate mass flux values, slightly higher ΔT_{wet} values were measured on average for upward flow tests than the corresponding downward flow tests. The difference was negligible at mass flux values > 1200 kg/m^2s.

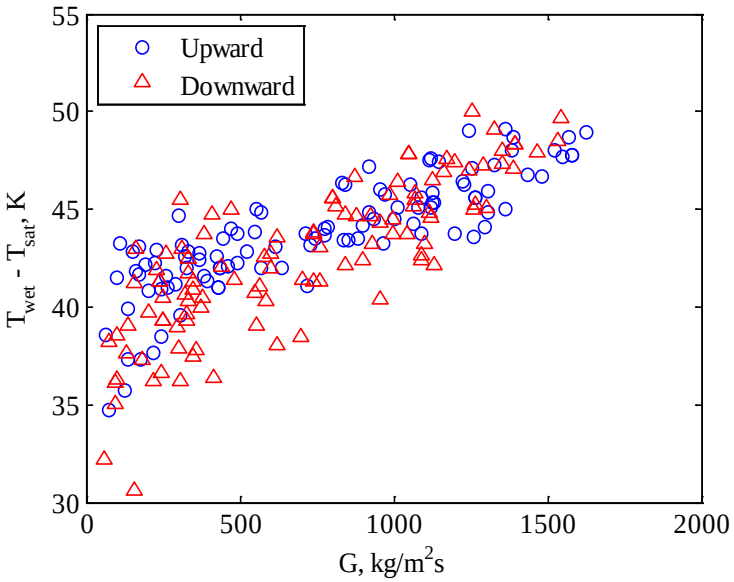

Figure 3 Rewet temperature minus the saturation temperature vs. the mass flux for both upward flow and downward flow.

Previous correlations found in the literature, listed in Table 1, were compared with the data. The results are shown in Figures 4-7, where the predicted T_{wet} value by each model is compared to the measured T_{wet} given in Figure 3, for upward flow only. Very similar results are obtained with the downward flow data, hence they are given here. In Figure 4, the correlations that are based on the hydrodynamic models all drastically over-predict T_{wet}. In Figure 5, those that are based on the thermodynamic models do fairly well at the low T_{wet} values, which correspond to the low flow rate tests, but only the correlation by De Salve and Panella does well over the entire range of data. This is because the De Salve and Panella correlation is the only thermodynamic model that accounts for the trend that higher mass fluxes cause higher T_{wet} values. The mean absolute error (MAE) also given in Table 1, calculated as $|\Delta T_{wet,calculated} - \Delta T_{wet,measured}|/\Delta T_{wet,measured} \times 100\%$, was the smallest for the De Salve and Panella correlation at 19%. The fact that it was developed from data with water and it works well with LN_2 data shows that it is a promising general-fluid correlation.

In Figure 6, the Bernardin and Mudawar model, that is based on bubble nucleation is compared with the data, the model uniformly underpredicts T_{wet} for all tests by 30 to 40 K. But it is important to note that the predictions by the Bernardin and Mudawar model do show a consistent trend with that of the data that provides the basis for building a new correlation to be presented in the next section. The comparisons of other models with the experimental data are shown in Figure 7. It can be seen that all three other models do not perform well as all three models are not sensitive to T_{wet}.

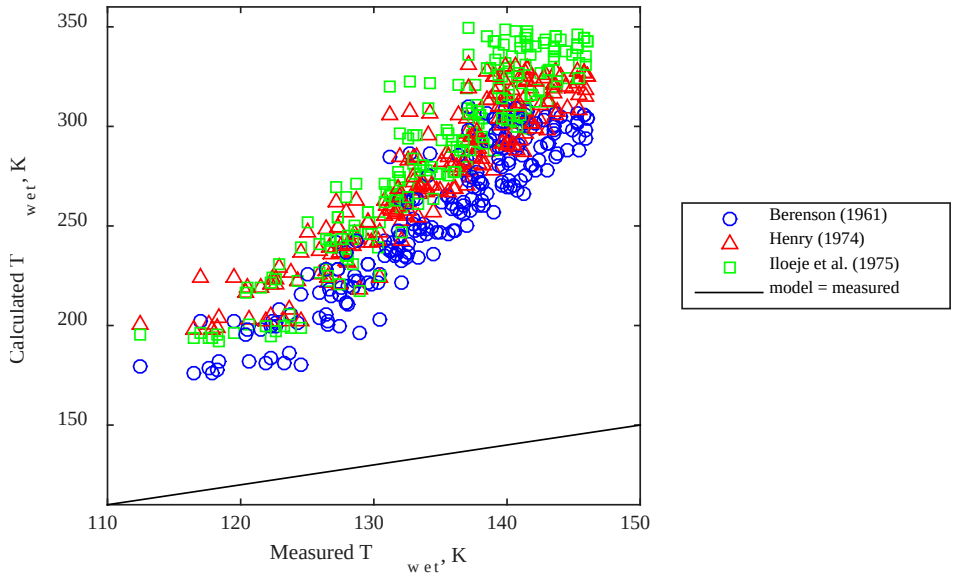

Figure 4 Current data compared to hydrodynamic models

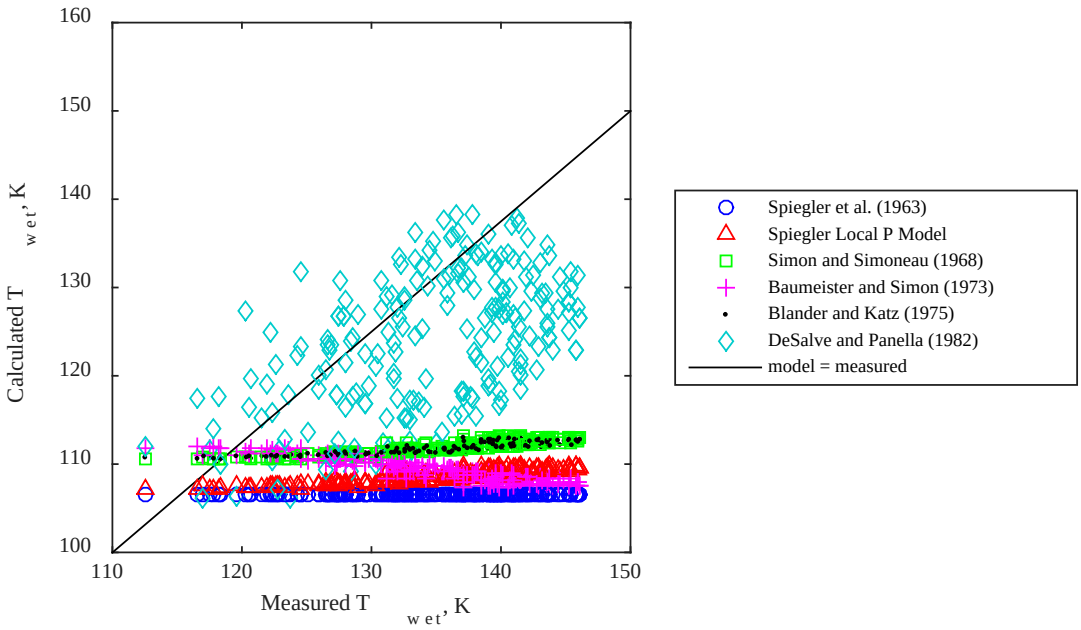

Figure 5 Current data compared to the maximum limit of superheat models

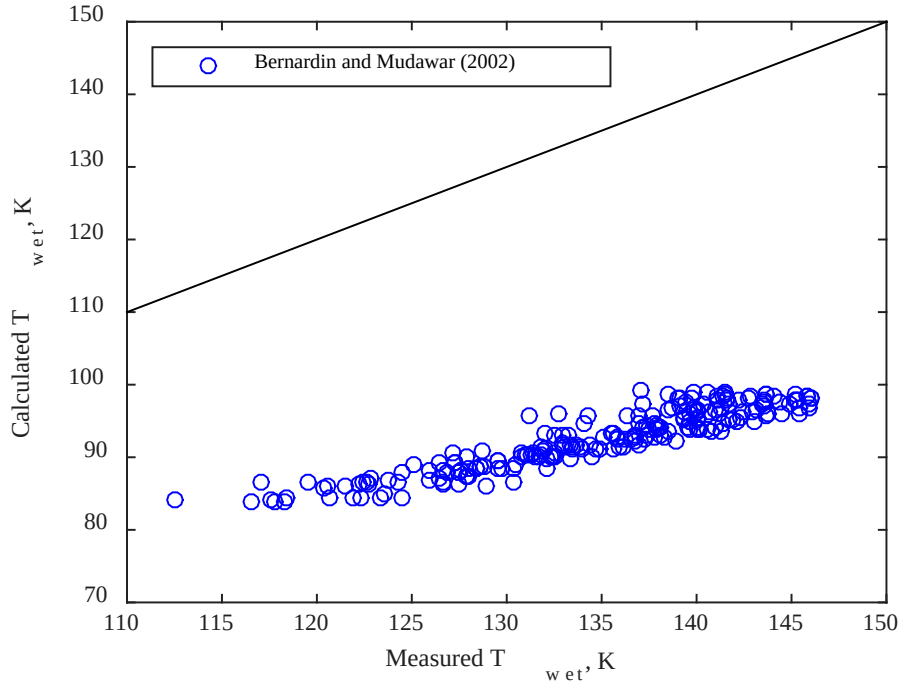

Figure 6 Current data compared to the bubble nucleation model

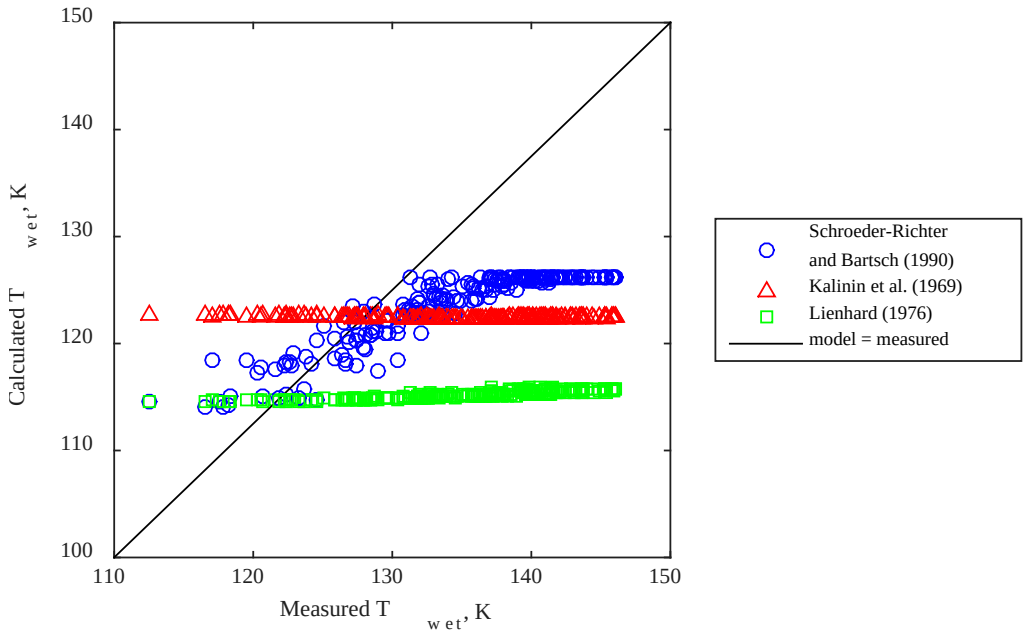

Figure 7 Current data compared to other models

Table 1. Previously reported rewet temperature correlations

Model Type	Author (Year)	Equation	MAE%
Hydrodynamic Theory	Berenson [7], (1961)	$T_{wet} = 0.127 \frac{\rho_v h_{lv}}{k_v} \left[\frac{g(\rho_l - \rho_v)}{\rho_l + \rho_v} \right]^{2/3} \left[\frac{\sigma}{g(\rho_l - \rho_v)} \right]^{1/2} \left[\frac{\mu_v}{g(\rho_l - \rho_v)} \right]^{1/3}$	277
	Henry [13], (1974)	$T_{wet} = T_{wet,Ber} + 0.42 \left[\beta h_{fg} / \left[C_{p,w} \left(T_{wet,Ber} - T_{sat} \right) \right] \right]^6 \left(T_{wet,Ber} - T_{sat} \right)$ where $T_{wet,Ber}$ is the rewet temperature calculated from the Berenson model and $\beta = \sqrt{\left(k_l \rho_l c_{p,l} \right) / \left(k_w \rho_w c_{p,w} \right)}$	326
	Iloeje et al. [14], (1975)	$T_{wet} = T_{sat} + 0.29 \left(T_{wet,Ber} - T_{sat} \right) \left(1 - 0.295 x_{eq}^{2.45} \right) \left(1 + 0.279 G^{0.49} \right)$	345
Maximum Limit of Superheat	Spiegler et al. [15], (1963)	$T_{wet} = \frac{27}{32} T_{cr}$	66
	Simon and Simoneau [20], (1968)	$T_{wet} = T_{cr} \left[0.13 P / P_{cr} + 0.87 \right]$, Units of Kelvin	53
	Baumeister and Simon [4], (1973)	$T_{wet} = \frac{0.844 T_{cr} \left(1 - \exp \left\{ -.52 \left[10^4 \left(\rho_w / N_w \right)^{4/3} \right] / \sigma \right\} \right) - T_{sat}}{\exp \left[3.06 \times 10^6 / \left(k_w \rho_w c_{p,w} \right) \right] \operatorname{erfc} \left[1751.5 \left(k_w \rho_w c_{p,w} \right)^{-1/2} \right]} + T_{sat}$	59
	Blander and Katz [28], (1975)	$J \approx 1.186 \times 10^{34} \left[\frac{d^2 \sigma}{M^3 B} \right]^{1/2} \exp \left[\frac{-1.2135 \times 10^{24} \sigma^3}{T_L (P_e - P_L)^2 \delta^2} \right] \approx 10^6$ $\delta \cong 1 - (\frac{d_G}{d}) + \frac{1}{2} (\frac{d_G}{d})^2$ d is liquid density, d_G is vapor density, M is molecular weight, σ is surface tension, P_e is equilibrium vapor pressure. The equation is implicitly solved for T_L	50.9
	De Salve and Panella [22], (1982)	$T_{wet} = T_{sat} + \frac{0.29 \left(0.844 T_{cr} - T_{sat} \right) \left(1 + 0.279 G^{0.49} \right)}{\exp \left[3.06 \times 10^6 / \left(k_w \rho_w c_{p,w} \right) \right] \operatorname{erfc} \left[1751.5 \left(k_w \rho_w c_{p,w} \right)^{-1/2} \right]}$	19

Bubble nucleation and growth	Bernardin and Mudawar [24], (2002)	$T_{sat}\exp\left[2\sigma\left(\nu_v-\nu_l\right)/\left(r_b h_{lv}\right)\right]=T_i+\left(T_l-T_i\right)\mathrm{erf}\left[r_b/\left(2\sqrt{\alpha_l t}\right)\right]$ (*) $AB\%(t)=\psi\frac{a_1}{a_2}\left\{\exp\left[-a_1 r_{\min}(t)\right]-\exp\left[-a_2 r_{\max}(t)\right]\right\}\pi r_{\max}^2(t)$ (**) $T_i=\frac{\left(k_w\rho_w c_{p,w}\right)^{1/2}T_w+\left(k_l\rho_l c_{p,l}\right)^{1/2}T_l}{\left(k_w\rho_w c_{p,w}\right)^{1/2}+\left(k_l\rho_l c_{p,l}\right)^{1/2}}$ These set of equations are implicitly solved for $T_l = T_{sat}$ that gives an average growth rate value of $\Delta AB\%/\Delta t$ = 0.05 %/μs a_1 and a_2 are empirical coefficients of the equation $n=a_1\exp(a_2 r_c)$ where n is the number of surface cavities per unit area per unit interval and r_b is the cavity radius. Values of a_1 = 4.597 and a_2 = -12.2 were given for nickel. These values were used in this study because it was thought that stainless steel would have similar surface cavity properties to nickel.	97.5
Others	Kalinin et al. [2], (1969)	$T_{wet}=T_{sat}+1.65\left[0.1+1.5\sqrt{\beta_w/\beta_l}+0.6\beta_w/\beta_l\right]\left(T_{cr}-T_{sat}\right)$	30
	Lienhard [27], (1976)	$T_{wet}=T_{sat}+T_{cr}\left[0.905-\left(T_{sat}/T_{cr}\right)+0.095\left(T_{sat}/T_{cr}\right)^8\right]$	46
	Lienhard [19], (1982)	$T_{wet}=T_{cr}\left[0.923+0.077\left(T_{sat}/T_{cr}\right)^9\right]+T_{sat}$	40
	Schroeder-Richter and Bartsch [26], (1990)	$h_{v,sat}(\mathrm{P}_l)-h_{l,sat}(\mathrm{T}_{wet})=\frac{1}{2}\left(v_{v,sat}(\mathrm{P}_l)-v_{l,sat}(\mathrm{T}_{wet})\right)\left(P_{sat}(\mathrm{T}_{wet})-\mathrm{P}_l\right)$ * The MAE is evaluated within the up limit of the model (T_{cr}=126k)	25 12*

4 New Correlations

4.1 Modified Bernardin and Mudawar Correlation

As mentioned in the previous section that the Bernardin and Mudawar model predicted the correct trend with that of the experimental data. So a new correlation can be built by making a proper correction. One of the main assumptions in the model is that the growth of bubbles off of the surface are hemispherical, an appropriate assumption for water on stainless steel. But for LN_2 the contact angle is very low, 7° or less. To account for this, the height of the bubble was changed from a hemispherical shape to a shallow dome shape with a contact angle of 7°. This changed the equation that determined the surface superheat temperature required to initiate bubble growth to:

$$T_{sat}\exp\left[2\sigma\left(\nu_v-\nu_l\right)/\left(r_b h_{lv}\right)\right]=T_i+\left(T_l-T_i\right)\mathrm{erf}\left[r_b\left(1+\cos\theta_c\right)/\left(2\sqrt{\alpha_l t}\right)\right] \quad (27)$$

where θ_c = 7°. Using this equation with the remaining equations in the table, the results agreed well with both the upward flow and downward flow data (shown in Figure 8 against upward flow data). However, an AGR value of $\Delta AB\%/\Delta t = 0.0473$ %/μs was found to agree best with the data instead of 0.05 which was reported in the paper. The MAE value was calculated as 8.5%. After examining the data, it was found that the model predicted an unanticipated relationship with pressure. It appeared that the model predicted an exponential increase with pressure, whereas the data showed that T_{wet} began to level off with pressure. A quadratic fit of the AGR with pressure, shown in Figure 10 , was used to obtain better results. The new model vs. downward flow data is shown in Figure 9. The MAE value was reduced to 6.1%.

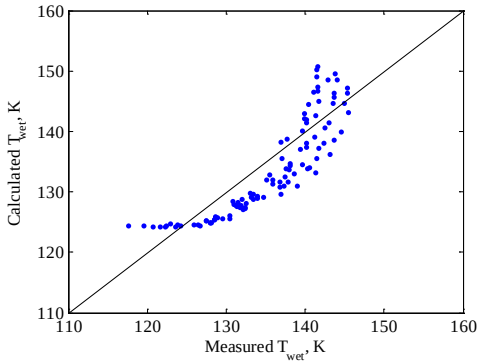

Figure 8 Modified Bernardin and Mudawar model comparison to vertical upward data. A low MAE value of 8.5% was acheived.

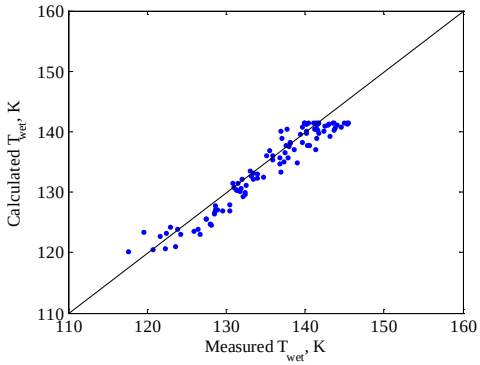

Figure 9 – Modified Bernardin and Mudawar model with updated AGR compared to vertical upward data, MAE = 6.1%.

4.2 Modified Baumeister and Simon Correlation

The De Salve and Panella model, which is a modification of the Baumeister and Simon model that takes into account the effect of mass flux, performed well against the current data set. However, it used the dimensional variable *G* in the correlation. To make a more robust correlation that will perhaps be applicable to more fluids including other cryogens like oxygen and hydrogen, we follow the same idea as De Salve and Panella but use the dimensionless Weber number to take into account the effect of fluid velocity. The Weber number has been shown to have a strong relationship with the physics of jet breakup from De Salve and Panella. The increase in rewet temperature due to mass flux is believed to be caused by the impingement of liquid slugs ejected from the liquid core. Thus the Weber number is likely a good measurement of the amount of rewet temperature increase due to liquid impingement. The new model takes the form:

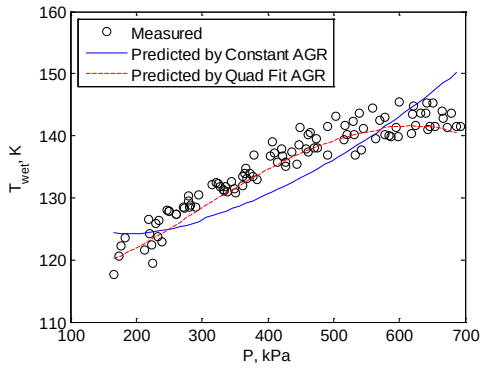

Figure 10 Rewetting temperature vs pressure with modified Bernardin and Mudawar model shown with AGR = 0.0436 and AGR quadratically fit to pressure. Data is from upward flow tests.

$$T_{wet} = \left\{ \frac{0.844 T_{cr} \left(1 - \exp\left\{\left[10^4 \left(\rho_w / N_w\right)^{4/3}\right] / \sigma\right\}\right) - T_l}{\exp\left[3.06\times10^6 / \left(k_w \rho_w c_{p,w}\right)\right] \operatorname{erfc}\left[1751.5 \left(k_w \rho_w c_{p,w}\right)^{-1/2}\right]} + T_l \right\} \left(1 + c_1 We_D^{c_2}\right) \qquad 28$$

The results worked well against the data, and a significant improvement over the De Salve and Panella correlation was obtained with a reduction in the MAE value from 19% to 7.5% against both the upward and downward flow data. Values of 0.060 and 0.208 were found for fitting coefficients c_1 and c_2, respectively. A plot of the new model against the 90° upward and downflow data is shown in Figure 11.

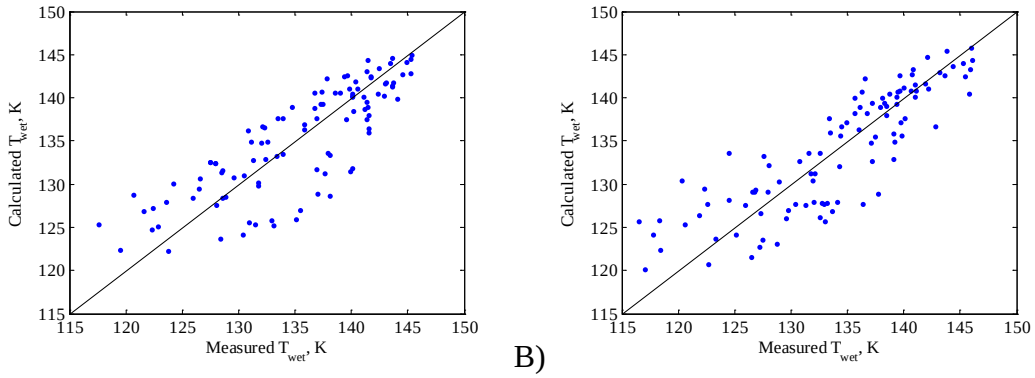

A) B)

Figure 11 Modified Baumeister and Simon model shown against A) upward flow data and B) downward flow data

5 Conclusion

The two modified correlations performed well over the entire dataset of LN_2 chilldown data. The physical mechanisms underlying each correlation are different, however. The actual physical mechanism for the rewetting phenomena has been continuously debated, however, it can be said with confidence that the rewet temperature for cryogenic pipe chilldown and even pool boiling cannot be described by the hydrodynamic theory first presented by Berenson [7] and later modified by others. To vet the legitimacy of the cavity actuation/bubble growth model by Bernardin and Mudawar [24] for LN_2, it would be necessary to visualize the Leidenfrost phenomena characterize the bubble coverage area and the surface cavity size distribution as it was done for room temperature fluids.

Acknowledgment

This work was funded by the NASA MSFC Space Launch System Advanced Development Project under Grant NNM13AA08G with Melinda Nettles as the Program Director.

References

[1] J. Carbajo, "A Study on the Rewetting Temperature," *Nuclear Engineering and Design,* vol. 84, pp. 21-52, 1985.

[2] Kalinin et al., "Investigation of the crisis of film boiling in channels, Two-Phase Flow and Heat Transfer in Rod Bundles," in *Proc. ASME Winter Annual Meeting*, Los Angeles, 1969.

[3] V. P. Carey, Liquid-Vapor Phase-Change Phenomena, 2nd ed., New York, NY: Taylor & Francis Group, LLC, 2008.

[4] K. J. Baumeister and F. F. Simon, "Leidenfrost temperature - its correlation for liquid metals, cryogens, hydrocarbons and water," *Trans. ASME, J. Heat Transfer*, Vols. 94-C, pp. 166-173, 1972.

[5] S. R. Darr, H. Hu, R. Shaeffer, J. N. Chung, J. W. Hartwig and A. Majumdar, "Numerical simulation of the liquid nitrogen chilldown of a vertical tube," in *53rd AIAA Aerospace Sciences Meeting*, Kissimmee, FL, 2015.

[6] S. R. Darr, H. Hu, N. Glikin, J. Hartwig, A. Majumdar, A. LeClair and J. Chung, "An experimental study on terrestrial cryogenic tube chilldown: II Effect of flow direction with respect to gravity," *International Journal of Heat and Mass Transfer*, 2016.

[7] P. J. Berenson, "Film boiling heat transfer from a horizontal surface," *Trans. ASME, J. Heat Transfer*, vol. 83, pp. 351-58, 1961.

[8] N. Zuber, "Hydrodynamic Aspects of Boiling Heat Transfer (thesis)," University of California, Los Angeles, 1959.

[9] G. Taylor, "The Instability of Liquid Surfaces when Accelerated in a Direction Perpendicular to their Plane," *Proceedings of the Royal Society of London*, Vols. A-201, p. 192, 1950.

[10] P. Berenson, "Technical Report: Transition Boiling Heat Transfer from a Horizontal Surface," Massachusetts Institute of Technology, Heat Transfer Laboratory, Cambridge, MA, 1960.

[11] L. Bromley, "Heat transfer in stable film boiling," *Chemical Engineering Progress*, vol. 46, pp. 221-227, 1950.

[12] E. Keshock and K. Bell, "Heat Transfer Coefficient Measurements of Liquid Nitrogen Drops Undergoing Film Boiling," *Advances in Cryogenic Engineering*, vol. 1970, pp. 271-282, 1969.

[13] R. E. Henry, "A correlation for the minimum film boiling temperature," *AIChE Symposium Series*, vol. 70, no. 138, pp. 81-90, 1974.

[14] O. Iloeje, D. N. Plummer, W. M. Rohsenow and P. Griffith, "An investigation of the collapse and surface rewet in film boiling in forced vertical flow," *Journal of Heat Transfer*, vol. 97, no. 2, pp. 166-172, 1975.

[15] P. Spiegler, J. Hopenfeld, M. Silberberg, C. Bumpus Jr. and A. Norman, "Onset of stable film boiling and the foam limit," *International Journal of Heat and Mass Transfer*, vol. 6, pp. 987-994, 1963.

[16] H. Temperley, "The Behavior of Water Under Hydrostatic Tension: III," *Proceedings of the Physical Society*, vol. 59, no. 2, p. 199, 1947.

[17] P. Spiegler, J. Hopenfeld and A. Norman, "Operating Conditions of Bubble Chamber Liquids," *Review of Scientific Instruments*, vol. 34, pp. 308-309, 1963.

[18] J. Lienhard and V. Schrock, "Generalized displacement of the nucleate boiling heat-flux curve, with pressure change," *International Journal of Heat and Mass Transfer,* vol. 9, pp. 355-363, 1966.

[19] J. Lienhard, "Correlation for the limiting liquid superheat," *Chemical Engineering Science,* vol. 31, no. 9, pp. 847-849, 1976.

[20] F. F. Simon and R. J. Simoneau, "Transition from film to nucleate boiling in vertical forced flow," 1969.

[21] J. Bernardin and I. Mudawar, "The Leidenfrost point: experimental study and assessment of existing models," *Journal of Heat Transfer,* vol. 121, no. 4, pp. 894-903, 1999.

[22] M. De Salve and B. Panella, "Analytical Model for Bottom Reflooding Thermal-Hydraulics in Circular Ducts and Comparison with Experimental Results," in *Heat Transfer in Nuclear Reactor Safety,* 1982.

[23] S. Yao and R. Henry, "An investigation of the minimum film boiling temperature on horizontal surfaces," *Journal of Heat Transfer,* vol. 100, no. 2, pp. 260-267, 1978.

[24] J. D. Bernardin and I. Mudawar, "A Cavity Activation and Bubble Growth Model of the Leidenfrost Point," *Journal of Heat Transfer,* vol. 124, pp. 864-874, 2002.

[25] A. Segev and S. Bankoff, "The role of adsorption in determining the minimum film boiling temperature," *International Journal of Heat and Mass Transfer,* vol. 23, pp. 637-642, 1980.

[26] D. Schroeder-Richter and G. Bartsch, "The Leidenfrost phenomenon caused by a thermo-mechanical effect of transition boiling: A revisited problem of non-equilibrium thermodynamics," *Fundamentals of Phase Change: Boiling and Condensation,* pp. 13-20, 1990.

[27] J. H. Lienhard, "Corresponding States Correlations of the Spinodal and Homogeneous Nucleation Limits," *Journal of Heat Transfer,* vol. 104, no. 2, pp. 379-381, 1982.

[28] M. Blander and J. Katz, "Bubble nucleation in liquids," *AIChE Journal,* vol. 21, no. 5, pp. 833-848, 1975.